Engineering Structures 46 (2013) 104–115

Contents lists available at SciVerse ScienceDirect

Engineering Structures

journal homepage: www.elsevier.com/locate/engstruct

Prefabricated floor panels composed of fiber reinforced concrete and a steel substructure

Lárus H. Lárusson *, Gregor Fischer, Jeppe Jönsson

Technical University of Denmark, Department of Civil Engineering, Brovej, Building 118, 2800 Kgs. Lyngby, Denmark

ARTICLE INFO

Article history:
Received 16 January 2012
Revised 7 June 2012
Accepted 27 June 2012
Available online 8 September 2012

Keywords:
Composite
ECC
Lightweight deck panel
Modular deck system

ABSTRACT

This paper reports on a study on prefabricated composite and modular floor deck panels composed of relatively thin fiber reinforced concrete slabs connected to steel substructures. The study focuses on the design, manufacturing, structural improvements and behavior of the floor systems during loading at the serviceability and ultimate limit states. The composite construction concept offers flexibility in the assembly process, the ability to adapt to various load and boundary requirements, and efficient utilization of material properties that result in a light weight prefabricated structural element.

The activities described in this paper are an extension of previous work where composite floor panels composed of light gauge steel joists were integrally cast with a thin-walled Engineered Cementitious Composite (ECC) slab. The main focus of the present study was to revise and improve the design detailing of these integrally cast deck panels and to modify them by providing individually cast anchor points in the precast ECC slab, which are subsequently used to attach a steel truss substructure.

Full-scale experiments were carried out to verify the structural behavior of the integrally cast panels and the modular panels with various substructure configurations along with comparison to analytical and numerical results.

© 2012 Elsevier Ltd. All rights reserved.

1. Introduction

1.1. Background

The motivation behind the project presented in this paper was to research and develop an alternative to current prefabricated floor systems with the goal of increasing production efficiency while reducing weight by using new and innovative building materials.

An increasing number of innovative structural floor systems both prefabricated and cast-in place have been previously implemented in the construction industry. The most commonly used prefabricated structural floor systems are hollow core decks (Fig. 1a) and double-T decks (Fig. 1b). Other semi prefabricated systems include filigrees (Fig. 1c), steel pan decks (Fig. 1d) and more recently biaxial hollow core decks (Fig. 2a), all of which are requiring casting of a concrete overlay at the construction site (in situ).

Design requirements and targets for prefabricated building products frequently include light weight, durability, implementation versatility, reduced construction time and cost. All of these requirements interact and affect each other and need to be addressed during the design process.

In this context, by utilizing the properties of new and innovative materials such as Fiber Reinforced Concretes (FRCs) in structural elements such as prefabricated floor panels allows for a more efficient construction process.

High Performance Fiber Reinforced Cementitious Composites (HPFRCCs) [1] such as Engineered Cementitious Composites (ECCs) have the ability to exhibit tensile strain hardening due to a specifically designed interaction between the cementitious matrix, the fibers and their interfacial bond. The strain hardening behavior of ECC is realized through an engineered interaction between a particular tensile stress–crack opening relationship and the formation of multiple cracking [2]. As a result of the ductile tensile load–deformation behavior of ECC, structural members can be designed with reduced sectional dimensions compared to those of normal steel reinforced concrete. This is possible due to the tensile strain hardening property of ECC, which has the same effect as steel reinforcement has in regular concrete and can reduce the amount of required reinforcement in a structural member, particularly in thin-walled structural elements.

In extension of previous work on Integrally Cast Panels (ICPs) (Fig. 3a), which examined thin-walled steel joists integrally cast into a thin ECC slab [3], the focus of this study was to further examine structural details of the ICP along with developing and testing a modular structure consisting of an ECC slab and a subsequently mounted steel truss substructure. The unique feature of the proposed modular segmented design are individual anchor points

* Corresponding author. Tel.: +45 3025 2774; fax: +45 4588 3282.
E-mail addresses: larus@byg.dtu.dk (L.H. Lárusson), gf@byg.dtu.dk (G. Fischer), Jej@byg.dtu.dk (J. Jönsson).

0141-0296/$ - see front matter © 2012 Elsevier Ltd. All rights reserved.
http://dx.doi.org/10.1016/j.engstruct.2012.06.035

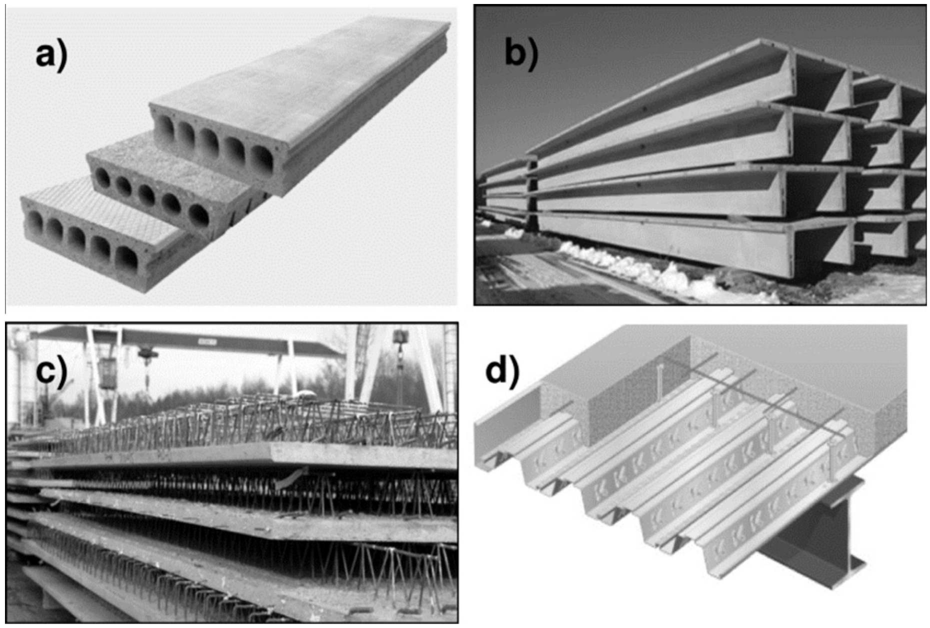

Fig. 1. Commercially available floor systems: (a) hollow core decks [19], (b) double T-deck elements [20], (c) filigree slabs with embedded lattice stirrup ridges [21], and (d) concrete on a pan deck supported by a steel joist [22].

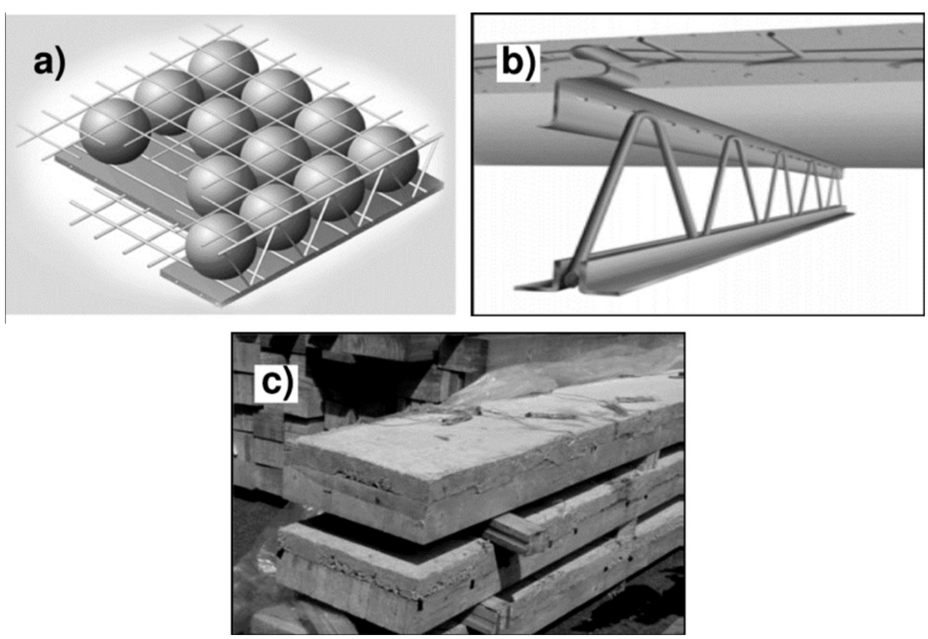

Fig. 2. Commercially available floor systems: (a) Bubble deck in Principe [7], (b) Hambro deck system in principle [11]. (c) Timber–concrete composite slab system [12].

integrally cast with the ECC slab, which are subsequently used to attach a steel truss substructure (Fig. 3b). By casting individual anchor points into the deck, the slab is allowed to shrink and deform independent of the substructure prior to assembly of the composite floor panel without causing shrinkage induced stresses and cracking and undesirable deflections of the deck panel during curing.

1.2. Overview of traditional prefabricated and semi-prefabricated floor deck systems

Prestressed hollow core decks (HCDs) [4,5] are widely used prefabricated elements suitable for most building types (Fig. 1a). The HCD have tubular voids running along the entire length of the element to reduce weight and consequently optimizing the tension and compression zones of the cross-section by removing ineffective concrete. The cross-section is utilized in compression by prestressing the element with high strength steel tendons to induce a clamping load that increases the active area and in effect the moment of inertia of the cross-section. As a result of reducing the weight and increasing the stiffness (moment of inertia), the deflections of the prefabricated element are decreased and allow a reduced structural height of the deck panels. The structural height of HCD elements typically ranges between 150 and 450 mm with a width of 1.2 m and a span ranging from 4 to 16 m depending on the expected loading and configuration.

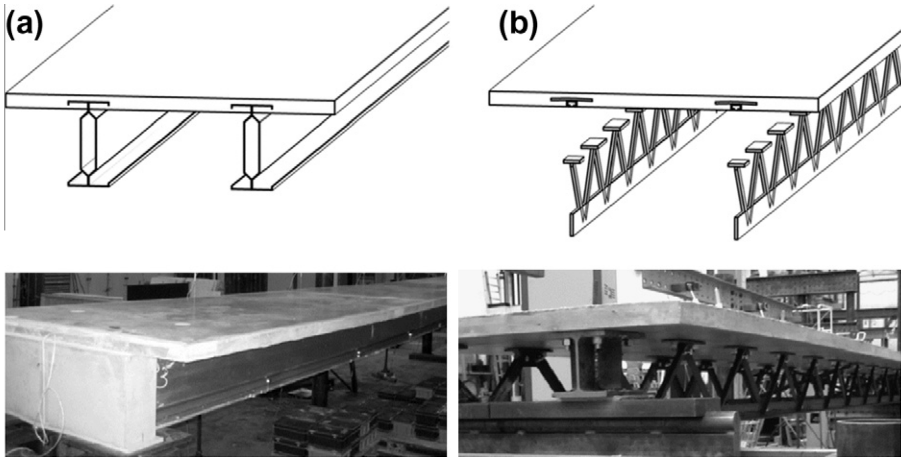

Fig. 3. (a) The integrally cast panel and (b) the modular concept.

Prestressed T- and double T-deck or slab elements (TD), also known as T- and double T-beams [5,6], are also widely used prefabricated elements (Fig. 1b). These elements are usually suitable for all building types but are more commonly used where loads are higher and spans are longer than normal (10–25 m spans). The structural heights of these elements are typically larger than other deck types as the structural concept of the TD is to utilize the distance between the compression zone and the tendons which are typically either prestressed or post-tensioned.

The casting procedure for factory produced elements such as HCD and TD allows for a relatively fast and accurate construction process where high product quality can be ensured. In this context, various techniques have been developed and are being implemented in the building sectors that combine the advantages of in situ casting and factory-made elements to optimize the design and further improve the implementation process.

Filigree plates (Fig. 1c) are one type of semi-prefabricated deck elements [7]. They combine regular Reinforced Concrete (R/C) slabs with prefabricated elements by utilizing the filigree as formwork during construction and as a structural component at the service load stage. A filigree slab is essentially the lower reinforcement grid of a regular R/C slab cast into a thin layer of concrete. In addition, lattice stirrup ridges on the filigree ensure a composite connection of the upper reinforcement and cast in place concrete with the lower prefabricated element. A number of different variations of the filigree concept have been developed with the purpose of eliminating the need for regular formwork and reducing installation and build time.

Biaxial hollow core deck systems, known as Bubbledeck® (Fig. 2a) or Cobiax®, are recently developed methods of constructing floor decks [8,9]. In principle, the concept is similar to that of traditional HCD. By utilizing the compression strength of concrete and tensile strength of the reinforcement and tendons, ineffective concrete can be removed and replaced with hollow plastic spheres (bubbles). Unlike traditional HCD, Bubbledeck is a biaxially spanning slab system, which carries load along both axes of its plane, similar to two way reinforced concrete slabs. It consists of a prefabricated filigree element with plastic spheres firmly locked in a reinforcement lattice while the lower parts of the spheres are cast in concrete to complete the Bubbledeck.

Reinforced concrete on a corrugated steel deck, also known as pan deck (Fig. 1d), performs in the same way as filigrees by integrating the steel pan as part of the reinforcement and formwork during construction [10]. It allows for thinner- and lighter decks compared to regular reinforced concrete slabs. Steel pan decking is widely used in high rise buildings with steel frames and is generally considered a short span system with max spans in the range of 4–6 m. Once these filigree or corrugated panel elements have been put into place, the upper reinforcement lattice and anchoring is finalized before the concrete slab is cast in place, allowing for a continuous floor.

Hambro composite concrete-steel floor system is yet another innovative concept (Fig. 2b) [11]. Structural components include a relatively thin reinforced concrete slab and a steel truss integrally cast into the slab. This system is currently being produced and marketed as an alternative to heavier floor systems.

Timber–concrete composite slab systems (Fig. 2c) are also used in practice [12]. They utilize the tension properties of timber combined with the compression strength of concrete to create relatively light and slim floor decks. The main benefits of such systems are the reduced dead load, allowing for longer spans and a rapid construction time.

Table 1 compares relevant characteristics of various structural floor systems to give a general schematic overview of the different

Table 1
Comparison of different deck types, approximated range of spans and dead loads. For comparison reasons most of the structural heights compared are in the same range.

Deck types	Height (mm)	Width (m)	Spans (m)	Self weight (kN/m^2)
Composite ECC[a], MP, ICP	325	1.2	6–12	1.3
Hambro D500TM	350	1.25	6–9	2.6
Hollow core 1	265	1.2	4–10	3.6
Hollow core 2	320	1.2	4–12	4.0
Steel pan, Ribdeck AL	200	0.6–0.8	4–6	4.3
Bubbledeck	285	1–3	8–12	4.6
T-section	500	1.4	10–25	5.5
R/C and reg. filigree	300	6–8/1–3	6–8	7.5

[a] The composite ECC deck panels that are the focus of this study.

systems including the composite ECC deck panels presented in this paper.

1.3. Material properties

Engineered Cementitious Composites (ECCs) is a fiber reinforced cementitious composite material, which exhibits strain hardening and multiple cracking up to relatively large inelastic deformations (see Table 2). The micromechanical design of ECC results in the ability to increase its tensile loading capacity after first crack formation, which is realized through particular interaction between fibers, cementitious matrix, and their interfacial bond. This results in multiple cracking during tensile loading with an intrinsically controlled crack width on the order of 200–300 μm at reaching the tensile strength [1,13] The strain hardening and multiple cracking properties of ECC distinguishes it from regular brittle concrete and conventional tension softening Fiber Reinforced Concrete (FRC) as illustrated in Fig. 4. The elastic and post crack inelastic behavior of ECC can be described as being analogous to that of metals with a similar elastic/plastic load deformation behavior.

ECC is composed of ingredients commonly used in concrete including cement, fly ash, sand, water, admixtures and fibers at a volume fraction of 2%. The lack of coarse aggregate in ECC results from the requirements imposed by the micromechanical design concept, which limits the allowable fracture toughness of the cementitious matrix and therefore limiting the maximum size of the aggregates. The Polyvinyl Alcohol (PVA) fibers used in this study are 8 mm long with a diameter of 40 μm and were developed for optimal performance in ECC and to meet the specific micromechanical requirements.

Due to the composition of ECC, shrinkage is more extensive compared to conventional concrete. Drying shrinkage of ECC has been found in related studies to reach 0.10–0.15% strain at 40–70% Relative Humidity (RH), which is approximately 80% higher than drying shrinkage deformations of normal concrete [14].

Due to the ductile nature of ECC, the composite interaction of ECC and steel reinforcement (R/ECC) is significantly different from the interaction of regular concrete and steel reinforcement (R/C) with a distinctly different post cracking stress distribution in the R/ECC as a result of the formation of multiple cracking instead of localized cracking [15]. This evenly distributed load transfer between the rebar-matrix interfaces makes the composite interaction of ECC and steel substantially more compatible than that in R/C [16].

2. Concept and design

The objective of the panel systems presented in this paper was to develop a lightweight, easy to install alternative to traditional and heavier prefabricated floor systems by implementing High Performance Fiber Reinforced Cementitious Composites (HPFRCCs) such as ECC.

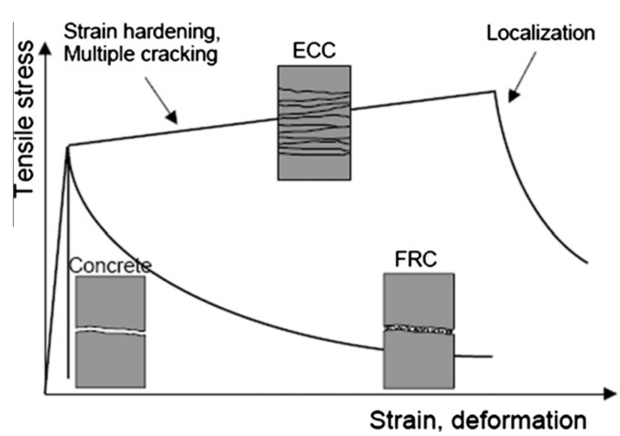

Fig. 4. Schematic tensile stress–strain behavior of cementitious matrices [1].

In previous studies [3], thin-walled steel profiles integrally cast with a thin ECC deck slab were fabricated and their structural behavior was investigated. These Integrally Cast Panels (ICPs) have been developed to meet some of the necessary criteria for floor decks according to codes of practice, such as loading capacity, deflection limits and dynamic response.

In continuation of this initial investigation on integrally cast panels, structural details of the segments support footings and cross bracing of the joists were addressed and a modular assembly of the ECC slab and the steel sub-structure was investigated. In these previous ICP studies, the casting forms and the thin-wall steel profiles were laid out in a shallow parabolic shape to compensate for shrinkage induced deformations of the deck element. The deformations previously observed in the integrally cast panels resulted from shrinkage of the ECC, due to which undesirable deflections and cracking had formed in the ICP decks.

The aim of the modular concept applied in this study is to separate the casting of the ECC deck slab and the attachment of the substructure by embedding anchors into the ECC slab, thus avoiding unfavorable deformations and cracking due to shrinkage typically encountered in the integrally cast floor panels [3]. By embedding individual attachment devices that later can be connected to a steel truss substructure, the modular system offers increased flexibility in assembly and transportation of the deck system. Moreover, the concept allows for high versatility in the substructure design and the ability to adapt to different required loading capacities and deflection limits as well as architectural requirements. Furthermore, the modular panel assembly allows for a precamber in the ECC slab of the modular floor panel to compensate for deformations due to self weight and creep during the initial use phase of the panel.

The flexibility of such a system lies in the design of the panel sub-structure where height, weight and architectural needs can be met without compromising structural integrity. The possibility of having wiring, ventilation and piping located within the structural height of the deck element allows the overall height of the floor construction to be reduced.

In the design of the modular panels, numerical models were implemented to aid in the dimensioning of the steel trusses. Two types of elements constitute the structural elements of the numerical models of the modular floor panel. The steel truss components were modeled as frame elements, while the ECC deck slab on top of the two trusses was modeled with shell elements (Fig. 5). The models were used to obtain static forces and natural frequencies for at the serviceability limit state and to predict the capacity at the ultimate limit state as well as to estimate the applied forces at failure observed during testing.

3. Analytical calculations of structural properties

To estimate the bending stress distribution in the panels, the following assumptions were made: a linear elastic strain distribution through the depth of the sections and plane sections remain plane after deformations (Fig. 6). Furthermore, assuming the deck panels are subjected to a uniformly distributed load, the bending stresses in the cross-section can be determined by employing the equivalent stiffness of the integrally cast- and the modular cross-sections. This equivalent stiffness ($E \cdot I_{Eq}$) is determined from the geometry and the material properties where E is the elastic modulus and I_{Eq} is the equivalent moment of inertia of the cross-section.

Assuming a linear elastic behavior of the materials, the resisting bending moment of the deck sections is estimated based on two

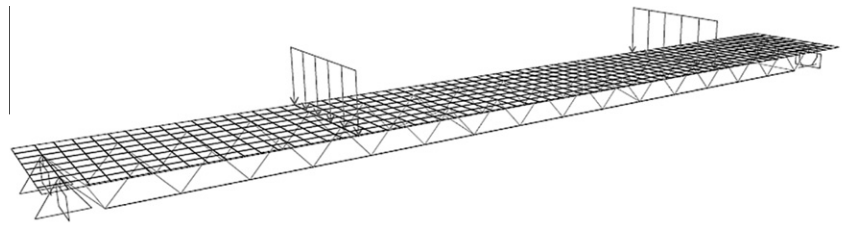

Fig. 5. Numerical model of modular panel, example of ultimate limit loading applied as line load over quarter points.

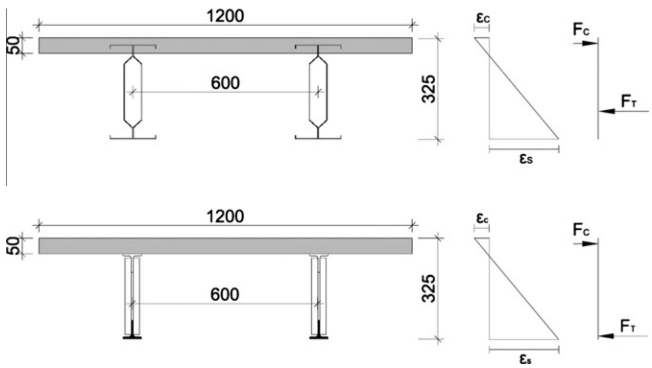

Fig. 6. Section view and assumed stress and force distribution of: (a) the Integrally Cast Panel (ICP), b) the modular deck panel (MP). Dimensions are given in mm.

failure criteria: the compression capacity of ECC is reached and yielding of the steel substructure. The contribution of the diagonals in the modular panel substructures is not taken into account in the analytical assessment of the bending stresses.

The deflections (v) of the panels are determined using equations for a simply supported beam with uniformly distributed load (q). For maximum deflection:

$$v = -q/(24 \cdot E \cdot I_{Eq}) \cdot (L^3/2 - 9L^4/16)$$

where q is the uniformly distributed line load and L is the span length of the deck element.

From the equation of motion, the natural frequency (f) of the system with a constant stiffness ($E \cdot I_{Eq}$) and mass (m) is determined as:

$$f = (n^2 \cdot \pi)/(2 \cdot L^2) \cdot ((E \cdot I_{Eq})/m)^{1/2} \quad n = 1, 2, 3, \ldots$$

To evaluate the damping ratio (ζ) of the structure, low damping is assumed, i.e. $(1 = \zeta^2)^{1/2} \approx 1$, and the damping ratio can be written as:

$$\zeta \approx \ln(u(t)/u)(t + T))/(2 \cdot \pi)$$

where $u(t)$ is the peak amplitude at time t and T is the time of one period [17].

4. Experimental program

In this study, the structural response of two integrally cast ECC-Steel joist deck panels (ICP1–ICP2) and four ECC modular deck panels (MP1–MP4) were experimentally evaluated. The overall dimensions of the deck panels are 1.2 m in width, an ECC slab thickness of 50 mm and an overall built height of 325 mm. The lengths of the panels are 8.2 m for the ICP and modular panels.

4.1. Test configuration and sequence

The deck elements were simply supported at both ends with a clear span of 8.0 m. At each end, the specimens were supported at two points in the transverse direction at a spacing of 0.6 m coinciding with the spacing of the trusses (Fig. 6).

Testing was carried out at two levels, at the serviceability limit state (SLS) and at the ultimate limit state (ULS). Loading at SLS was applied to the panels by a uniformly distributed line load over the 8.0 m span resulting in an equivalent area load of 4.08 kN/m^2. The distributed loading was applied in four steps at increments of 1.02 kN/m^2 at each step. The loads were applied in a line-load configuration directly above the trusses as the objective of these tests was to examine the behavior of the deck element in its longitudinal direction. During SLS loading, the dynamic response of the panels was measured by inducing a vibration in the deck elements and measuring its decay. From the obtained data the natural frequency and damping ratio were determined for each load increment (0–4.08 kN/m^2).

To evaluate the behavior of the floor panels at ULS, a four point bending configuration was used consisting of two point load couples (or transverse line loads) positioned on the deck at 2.0 m ($^1/_4$ L) and 6.0 m ($^3/_4$ L) relative to the 8 m span (Fig. 5) to induce a bending moment. Loading at ULS was increased gradually until failure occurred.

4.2. Specimen configuration

In constructing the ICP decks, four thin walled steel joists (cold-formed sigma profiles) (Fig. 6a), which constitute the substructure of each panel, were positioned in the bottom of the ECC deck slab (Fig. 3a). The steel joists are 300 mm high, 70 mm wide and have a thickness of 2.66 mm and a yield strength of 350 MPa. The thin walled profiles are embedded 25 mm into the 50 mm thick ECC deck slab resulting in an overall structural height of 325 mm. To ensure sufficient shear strength in the connection between the steel joists and the ECC slab, cut-outs in the steel profiles were made in the top part along the length of the profiles that connects to the slab (Fig. 7). Furthermore the ICP were cast with a slight

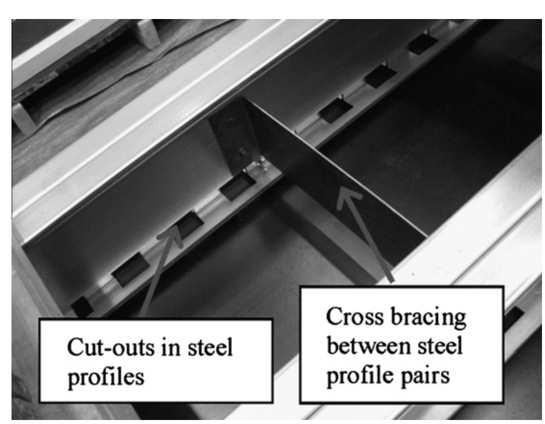

Fig. 7. Cut-outs in the steel profiles and cross bracing between steel profile pairs before ECC was cast.

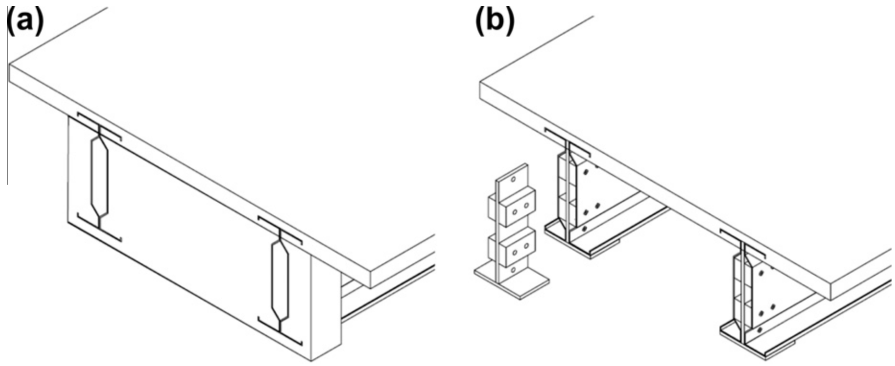

Fig. 8. A visual comparison of (a) Integrally Cast Panel 1 (ICP1) and (b) Integrally Cast Panel 2 (ICP2).

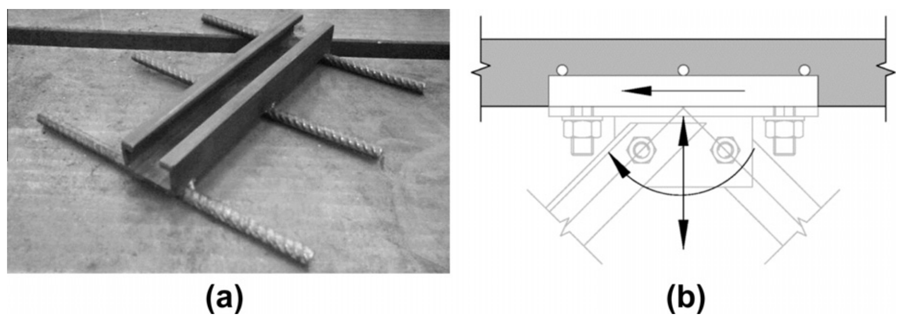

Fig. 9. (a) Cast-in anchor. (b) Resultant forces expected in cast-in anchor, forces shown in vertical and longitudinal direction.

curvature to account for shrinkage in the ECC and to create a negative deflection over the length of the panel. Structural improvements to the ICP design from the previous study [3] included cross bracing between the two pairs of steel joists (Fig. 7) and strengthening of the support footings. Difference in the structural detailing of the support footings separate the two ICP panels: ICP1 has the integrally cast steel joists confined in a block of ECC while the design of ICP2 features a steel strengthening element located between the steel profiles at the support (Fig. 8).

The modular floor slabs were manufactured with cast-in anchors (Fig. 9) positioned at the bottom of the ECC slabs, which are subsequently used to connect a steel truss assembly to the underside of the floor slab resulting in a complete composite deck element.

Due to the small thickness of the ECC slab ($t = 50$ mm), no suitable commercially produced cast-in place attachments were available and had to be custom fabricated to fit within the shallow depth of the ECC slab. To make the cast-in anchors, a system of interlocking steel channels and matching bolts was used to secure the channel segment firmly in the ECC slab with transverse anchor bars welded to the bottom of the channel (Fig. 9). To further increase the connection of the support footings to the ECC slab at the end of the floor segment, two channels were used for each anchor (Fig. 10). The geometry of the cast-in anchors was based on expected forces at the critical anchor points according to a numerical model of the composite panel.

The dimensions of the modular deck panel substructure (steel girders) were determined to have a height of 275 mm, resulting in a total structural height of 325 mm of the composite panel.

Four different steel truss configurations for the Modular Panels (MPs) were tested; specimens MP1, MP2, MP3 and MP4. In MP1, MP2 and MP3, the same ECC slab was used and re-used, while a second ECC slab (identical to the first slab) was used in MP4. Furthermore, the steel grade of the trusses in MP1, MP2 and MP3 was S235 while the steel grade in MP4 was S350.

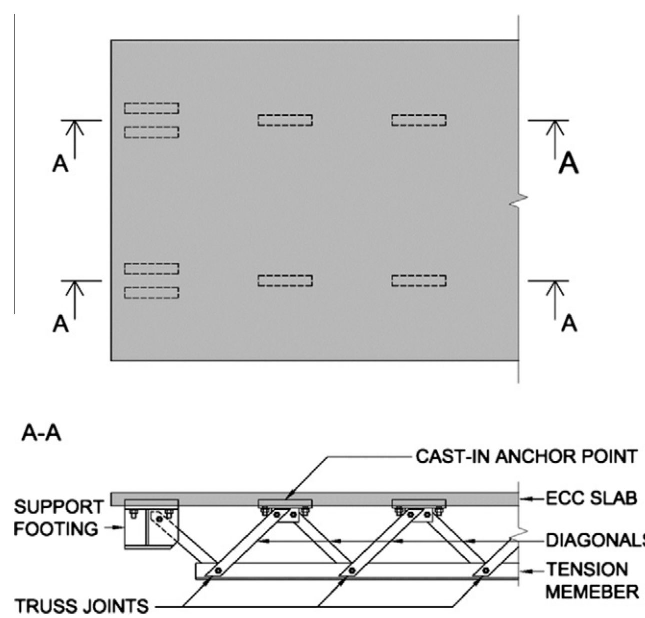

Fig. 10. (a) Plan over-view of the modular deck, (b) longitudinal cross-section of truss structure connected to ECC deck panel.

The first steel truss configuration in specimen MP1, was composed of $60 \times 60 \times 7$ mm steel T-profiles as the tension member and $40 \times 20 \times 4$ mm L-profiles as the diagonals. After testing of specimen MP1, the steel truss substructure was modified by replacing the diagonals of both trusses (9 on each end) with stronger $50 \times 50 \times 6$ mm L-profile diagonals (specimen MP2). After testing of specimen MP2, the tension member of the trusses were replaced with a larger $80 \times 80 \times 9$ mm T-profile resulting in specimen MP3. The steel trusses for specimens MP1, MP2 and

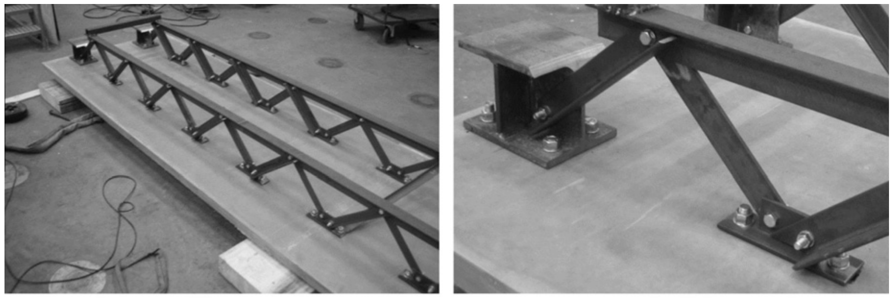

(a) (b)

Fig. 11. (a) Steel truss assembly. (b) Bolted connection to ECC slab.

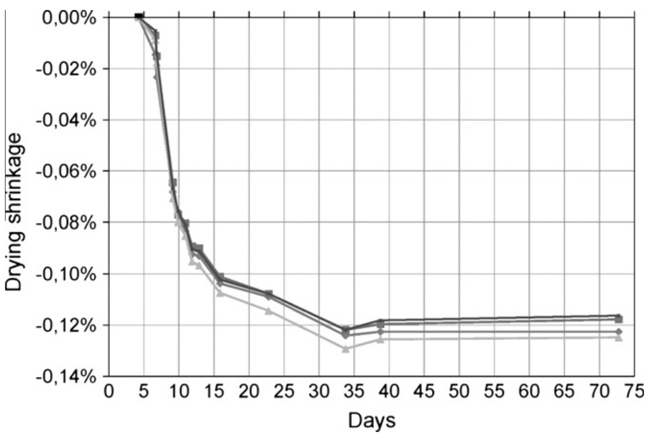

Fig. 12. Drying shrinkage of ECC over a period of 72 days.

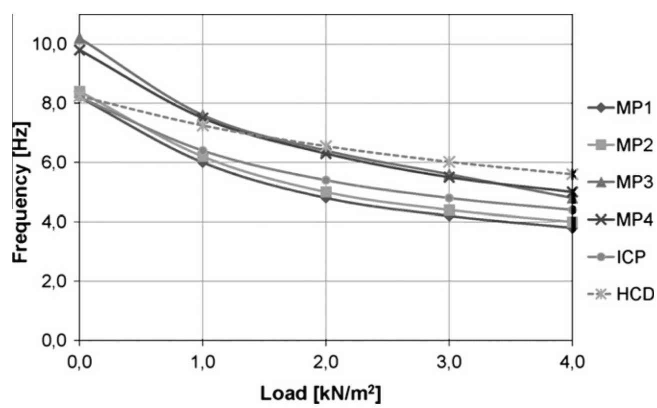

Fig. 14. The measured natural frequency as a function of applied service load.

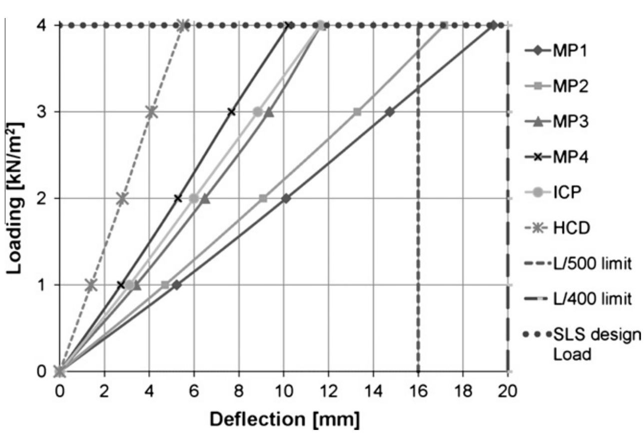

Fig. 13. Comparison of mid-span deflection of specimen MP1, MP2, MP3, MP4, ICP and HCD as a function of the applied load.

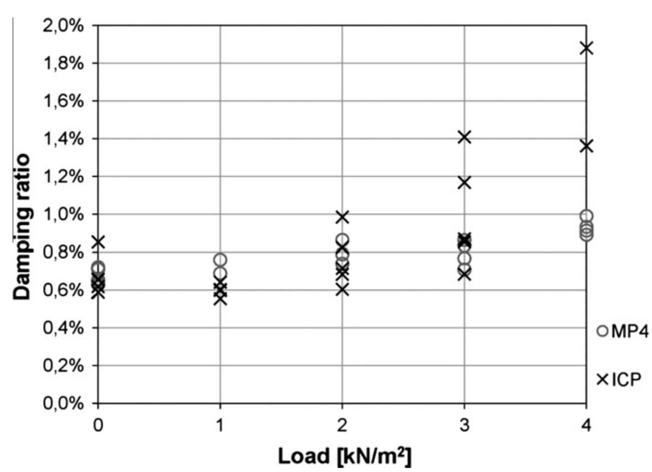

Fig. 15. Measured damping ratios for specimens MP4 and ICP as a function of additional live load.

MP3 were bolted together using M12 steel bolts, thus allowing for changing and replacing individual truss elements (Fig. 11). The truss-joint connections which connect the truss to the cast-ins in the slab were fabricated using the $60 \times 60 \times 7$ mm T-profiles (Fig. 9 b and Fig. 11).

Based on the experience from testing of specimens MP1, MP2 and MP3 at the service- and at ultimate state, the substructure connections of specimen MP4 were welded together using a 80×20 mm plate profile as the tension member, 40×8 mm plate profiles as tension diagonals, and $40 \times 40 \times 4$ mm RHS profiles as compression diagonals. The 40×8 mm plate-profile was also used to fabricate the truss-joint connections. As a conclusion to testing and revising of preceding designs (specimens MP1, MP2 and MP3), specimen MP4 was designed and built to have a moment resistance of 260 kNm, equivalent to that of a hollow core deck with the same span and similar structural height.

To ensure that the shear forces in the truss structures at the end-supports did not transfer directly into the thin ECC slab, the supports-footings were designed as rigid blocks made from 200 mm long HE160B steel profiles (two for each truss). These

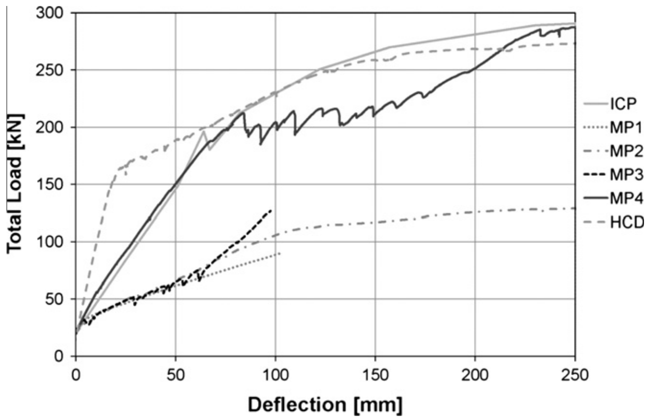

Fig. 16. Deflection at mid-span as a function of the total load of specimens MP1, MP2, MP4, ICP and the hollow core deck panel (HCD). Loading starts at 20 kN due to test configuration.

support footings were secured to the embedded cast-in anchors located at the ends of the deck element (Figs. 10 and 11b).

4.3. Material properties

Material tests were carried out to evaluate the mechanical properties of the ECC, including compressive strength, modulus of elasticity and drying shrinkage deformations. To insure analog development of the material properties of the test specimens to those of the actual panel specimen, all material specimens were cured in the same way as the panel specimens, i.e. at the same temperature and humidity. The compressive strength f_{ck} of the ECC on the day of testing was found to be 60 MPa with an elastic modulus of E_{cm} = 18 GPa. In addition, the drying shrinkage of the ECC was measured over a 68 day period using 270 mm long, test specimens with a cross-section of 25×25 mm^2. The results show that the drying shrinkage strain is approximately 0.12% after 30 days (Fig. 12) which is in good agreement with previously reported data [14], which showed drying shrinkage deformations of ECC to be 0.12% at 50–60% RH.

4.4. Experimental observations

4.4.1. Testing at serviceability limit state (SLS)

The specimens were subjected to a number of loading schemes to evaluate their structural behavior at the serviceability state, i.e. deflection, internal force distribution and dynamic response. For SLS loading, the deflection measurements were determined during the un-loading phase, i.e. the specimen was loaded with the full 4.0 kN/m^2 before being unloaded at increments of 1.0 kN/m^2 while measurements were taken. By doing so, any slip that occurs at this load level does not influence the measurements during unloading.

Due to virtually identical test results for ICP1 and ICP2 during SLS testing, results are shown for both specimens collectively as ICP.

A load deflection diagram for all specimens during SLS loading is shown in Fig. 13 and for comparison, a load deflection response of a hollow core deck with similar structural height is also shown.

The ICP specimens deflected 2.9 mm at mid-span for each 1.0 kN/m^2 applied, MP1 deflected 4.9 mm, MP2 deflected 4.3 mm, MP3 deflected 2.9 mm and MP4 deflected 2.5 mm at each load increment. All specimens except MP3 showed a linear load–deflection response during SLS loading while all specimens deflected less than the L/400 limit of 20 mm (Fig. 13).

Strain gauges placed on selected truss members of the modular substructure monitored the strain and consequently the stresses in elements of the steel substructure could be assessed during testing. The obtained stress and equivalent force distribution in truss structures MP1, MP2 and MP3 during SLS loading was in good agreement with the expected distribution found analytically and numerically.

Accelerometers positioned at the mid span of the deck panel were used to assess the dynamic response of the structure. The natural frequencies and damping ratios of the deck panels were measured by inducing a vibration in the decks and measuring its decay (Figs. 14 and 15). The natural frequency of specimens MP3 and MP4 was approximately 10 Hz at 0 kN/m^2 and 5 Hz at 4 kN/m^2 applied loading, which is 30% higher than that for specimens MP1 and MP2 at 0 kN/m^2 and 25% higher at 4 kN/m^2 (Fig. 14). The difference is a result of the changes made to the tension member and consequently increased effective stiffness of specimens

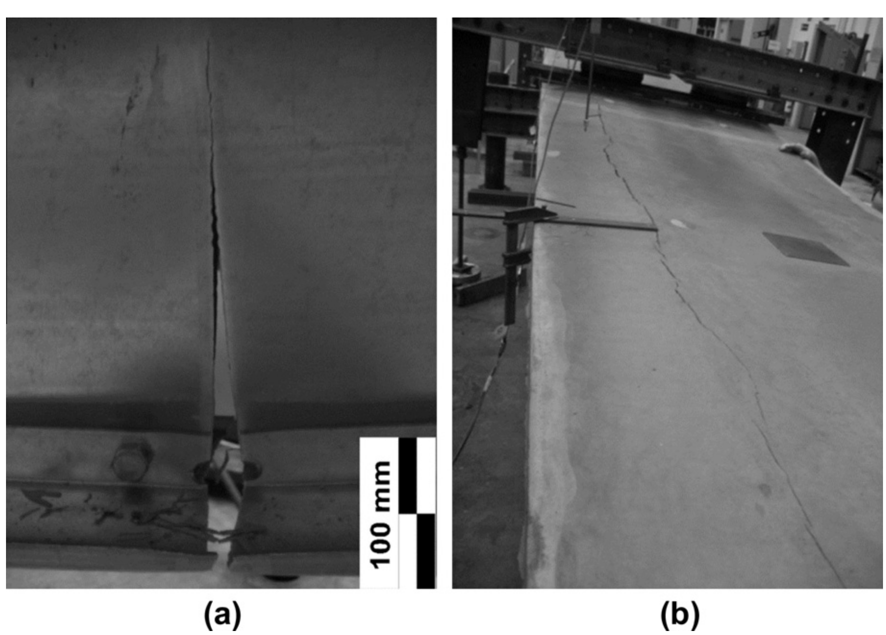

Fig. 17. Failure of specimen ICP1, (a) crack in the steel substructure and (b) a subsequent failure of the ECC deck.

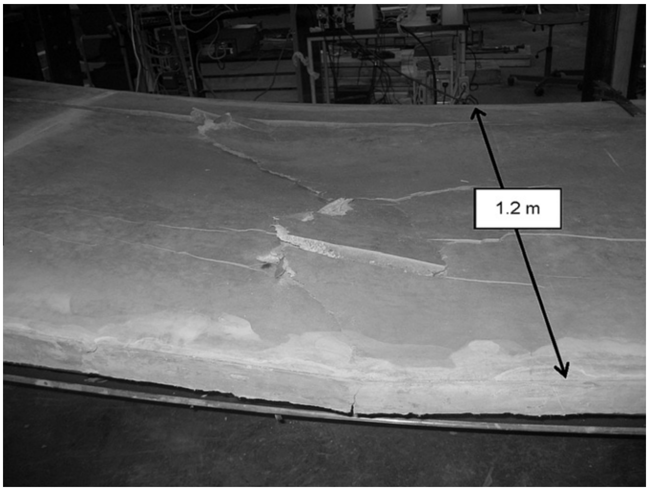

Fig. 18. Compression failure at mid-span of ICP2.

Fig. 19. Buckling of compression diagonals in specimen MP1.

MP3 and MP4. The increase in the natural frequency between the different specimens is directly related to the increase in stiffness of the composite panels and inversely related to its mass and applied load.

Due to the unknown effect of slip in the bolted connections of MP1, MP2 and MP3 on the damping measurements, the results from these tests were disregarded. Results from testing of ICP and MP4 are shown in Fig. 15. The damping ratio for the ICP specimens was found to be in the range of 0.6–1.8% and 0.6–1.0% for MP4 depending on the load arrangement. The damping ratio appears to be dependent on the change in mass and increasing as more loading is applied, indicating at increasing loads more damping mechanisms are activated in the specimens.

4.4.2. Testing at ultimate limit state (ULS)

During the ULS testing procedure, the deflections and load values were monitored along with strains of the tension member and selected diagonals of the steel trusses. The total load applied versus mid-span deflection for all specimens is shown in Fig. 16.

Specimen ICP1 reached a total load of 276 kN before one pair of the thin walled steel profiles fractured and the testing was terminated. The crack initiated and propagated from a small pre-existing hole close to the tension flange at mid-span resulting in a failure of the deck panel (Fig. 17).

Testing of specimen ICP2 was terminated after a compression failure occurred in the ECC slab, observed as a compression – sliding crack across the deck element at mid-span (Fig. 18). Prior to ultimate failure, a crack had formed over the length of the ECC deck slab at the interface of one of the embedded steel profiles, starting at mid-span and propagating to both ends. The total load ultimately reached 292 kN with a mid-span deflection in excess of 500 mm before failure occurred.

At a total load of 90 kN, testing of specimen MP1 was terminated when buckling of the compression diagonals occurred close to the end supports of the deck element due to shear (Fig. 19). Buckling of the diagonals was accompanied by twisting of the tension member of the truss structure due to eccentric positioning of the diagonal members relative to the longitudinal centerline of each truss; this detail was revised in subsequent specimens MP2, MP3 and MP4.

Testing of specimen MP2 was terminated when mid-span deflections exceeded 500 mm in a parabolic shape (Fig. 20). The tension member yielded between the quarter-points (points of loading) and ultimately reached 140 kN total applied load before testing was discontinued (Figs. 16 and 20). After testing, the ECC slab showed limited cracking, mainly propagating from the cast-in anchors directly below the point of loading, while multiple flexural cracking was observed at mid span (Fig. 21).

After testing of specimen MP2, the yielded tension members were replaced with profile members with a larger cross-section before the panel was reinstalled and tested as specimen MP3.

Testing of specimen MP3 resulted in an abrupt failure of the deck element due to shearing in the bolts connecting the diagonals of the steel truss. The total load reached 126 kN before shear failure occurred while slip in the bolted connections was apparent in the load–deflection graph (Fig. 16) as small drops in the load during ULS loading of specimen MP3. Slipping is observed up to about 70 mm deflection, above which no slip is observed and the load-deformation response becomes linear up until failure.

Specimen MP4 reached a total load of 291 kN before the test was terminated when the specimen ruptured and the substructure yielded directly below the points of loading (quarter points) (Fig. 22). At ultimate load, the specimen reached a mid-span deflection of 282 mm before structural failure occurred, resulting

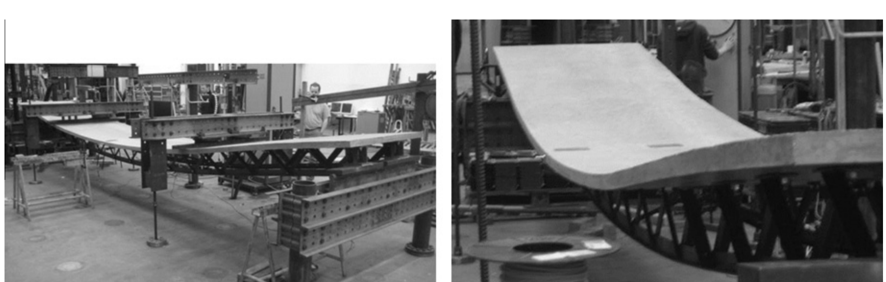

(a) (b)

Fig. 20. Deformed shape of specimen MP2 during (a) and after (b) ULS loading.

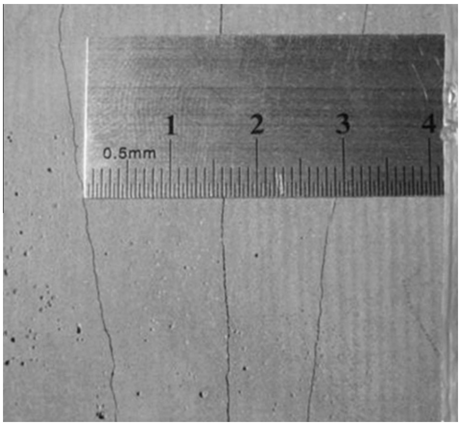

Fig. 21. Example of resulting cracks after ULS loading, figure shows multiple flexural cracks on bottom of ECC deck at mid-span.

Fig. 22. A combination of compression and flexural failure during ULS testing of specimen MP4.

in a reduced load carrying capacity. It was observed that the interlocking connections between the truss substructure and the anchor points next to the support footings had slipped, causing a crack to form directly above the support footings as well as bending of the connecting tension diagonal (Fig. 23).

Fig. 23. Excessive deformations at support due to slip in interlocking connection between truss and anchor point.

5. Discussion

The design criteria for the composite ECC deck panels included the loading capacity, a ductile failure mode by yielding of the steel substructure during ULS loading, a deflection limit, and a limited natural frequency (eigenfrequency) during SLS loading.

To evaluate these criteria, an experimental program was employed for the Integrally Cast Panel (ICP) and the Modular Panel (MP).

The concept of the Integrally Cast Panels (ICPs) and the Modular Panels (MPs) has numerous advantages over currently used prefabricated elements, most importantly the superimposed load to weight ratio (Table 1).

The ICP offers a simple construction concept, where lightweight steel profiles are joined directly with ECC slab to form a deck element, while the modular construction concept with the embedded anchors resolved some of the technical issues encountered in the ICṔs specifically the shrinkage induced deformation of the panels. The Modular Panels (MPs) offer the possibility to assemble the panels after drying shrinkage deformations in the ECC slab occur, which results in a significant reduction of the required precamber of the panels prior to installation and testing.

The purpose of the experimental program described in this paper is to analyze the structural behavior of the panel concept and to revise and improve the design through a trial and error methodology. The revised design obtained from these tests will serve as a foundation for a more detailed study in order to potentially commercialize the thin ECC floor panel concept (see Table 2).

5.1. Serviceability limit state

The measured deflections of the deck panels during SLS loading were all found to be below the required limit of L/400 (20 mm), furthermore all but deck panels MP1 and MP2 were below L/500 (16 mm) (Fig. 13). Furthermore the linear load–deflection responses in Fig. 13 indicate a full composite interaction of the deck slab with the substructure. While the analytical results for the modular panels (MP1–MP4) were consistently higher than the predicted results obtained from the numerical models, all of them are in good agreement with the experimental results (Table 3).

The natural frequencies of the panels (without additional loading) were measured to be in the range of 7.1 Hz (for MP1)–8.2 Hz (for ICP) and 3.8 Hz (for MP1)–5.0 Hz (for MP4) for the decks loaded with 4.0 kN/m^2 (see Fig. 14 for detailed results).

The decrease in deflection and increase in dynamic response between specimens MP1–MP4 and the ICP specimens relates directly to the increase in equivalent stiffness of the specimens. Due to the low weight of the composite panels, any superimposed loading is significant considering the low self weight of the specimens. Therefore, any additional weight will decrease the natural frequency of lighter deck systems proportionally more than for heavier, conventional deck systems. By alternating the position and the cross-sectional area of the tension member, a desired reduced deflection and natural frequency can be achieved to meet a wide range of design requirements on the static and dynamic performance of the composite ECC floor panels. Moreover, by optimizing the cross-section of each part in the steel substructure, the self weight

Table 2
Properties of ECC.

Flexural strength	16 MPa
Tensile strength	4–6 MPa
Tensile strain capacity	3–4%
Compressive strength	60 MPa
Modulus of elasticity	18 GPa
Density	2000 kg/m^3

Table 3
Comparison of: mid-span deflections, natural frequencies and mid-span stresses from analytical results (Ana.), numerical results (Num.) and actual measurements (Meas.) during SLS testing. Stresses are shown for a 4.0 kN/m^2 loading.

	Specimen MP1			Specimen MP2			Specimen MP3			Specimen MP4			Specimen ICP		
	Ana.	Num.	Meas	Ana.	Num.	Meas	Ana	Num.	Meas	Ana.	Num.	Meas	Ana.	Num.	Meas
Deflection (mm)															
At 4.0 kN/m^2	17.9	15.7	19.4	17.9	15.2	17.2	14.2	9.9	11.7	12.8	9.6	10.2	10.8	–	12.8
Span/defl.	447	510	412	447	526	465	563	808	684	625	833	784	741	–	625
Frequency (Hz)															
At self weight	7.23	8.12	8.20	7.10	8.22	8.40	7.74	9.85	10.20	7.97	9.99	9.85	9.5	–	8.1
At 4.0 kN/m^2	3.39	–	3.80	3.37	–	4.00	3.76	–	4.80	3.93	–	5.00	4.7	–	4.5
Stresses (MPa) at 4.0 kN/m^2 loading															
σ_{ECC}	4.7	3.8	–	4.7	3.8	–	5.2	3.2	–	5.6	3.2	–	1.6	–	–
σ_S	149.5	114.2	143.7	150.8	114.0	132.8	108.4	64.1	70.9	105.8	48.7	–	121.0	–	–

of the panels can be further reduced without compromising performance.

The measured decay of the free vibrations of the deck panels or damping ratios were found to be 0.6–1.0% for MP4 and 0.6–1.8% for ICP depending on the applied load (Fig. 15). As an example, according to CEB bulletin on vibrations in structures [18], the damping ratios found in the testing program correspond to those expected in composite sport and dance floors where the damping ratios have a minimum value of 0.8% and a maximum value of 2.5%.

Strain development in selected members of the truss structures of modular deck panels MP1, MP2 and MP3 were monitored during testing to verify the analytical and numerical predictions. In Table 3, a comparison of the equivalent stresses in the tension member (σ_S) and in the deck slab at mid-span (σ_{ECC}) is shown for all deck panels. The predicted diagonal forces obtained from the numerical models of MP1, MP2 and MP3 at SLS loading were all similar, whereas the values for MP4 were about 10–15% lower. The measured values in the diagonal members were consistently higher than the numerical predictions and rather scattered. The inconsistency of the measured force-distribution is most likely due to several factors including: inaccuracy in the fabrication of the individual truss elements, bolted connections, placement of strain gauges and precamber procedure, i.e. how the whole structure was assembled to create a negative deflection of the panels. As a result, the critical compression diagonals in the truss structure of MP1 (which ultimately failed due to bucking) were measured to have reached 85% of their theoretical buckling load at SLS loading of 4.0 kN/m^2.

At a 4.0 kN/m^2 loading of the composite panel, the load in the tension member of specimens MP1 and MP2 reached 55% of the yielding capacity of the steel while only utilizing 5% of the compression strength of the ECC slab. Equivalently, specimens MP3 and MP4 reached 20% of the yielding capacity of the tension member while utilizing about 10% of ECC compression capacity. To ensure a ductile failure mode at the ultimate limit state, the yielding capacity of the tension member of the truss structure must be lower than the compression capacity of the ECC slab as has been shown for MP2, MP4, ICP1 and ICP2 (Fig. 16).

5.2. Ultimate loading

Besides the structural detailing of the support footings, specimens ICP1 and ICP2 are identical and test results were are very similar, accordingly. The thin-walled steel profiles for both ICP1 and ICP2 started to yield at a total load of about 200 kN (equivalent to an area load of 21 kN/m^2) and continued to yield up to relatively large deflections of the specimens.

Specimen ICP1 failed unexpectedly when one pair of the thin-walled steel joists failed in tension (Fig. 17a). The failure caused a crack to form in the ECC deck slab immediately above the un-cracked profiles (Fig. 17b). This abrupt failure of the steel profiles resulted in a shift in the force distribution of the deck specimen causing the crack to form between the transversely protruding edge of the steel profile and the rest of the deck slab (Fig. 17b).

ICP2 reached a total load of 292 kN, equivalent to an area load of 30 kN/m^2, before its load carrying capacity was reached. Due to the large deflections in the deck panel, the tension and compression components of the cross-section associated with the moment of the deck panel also have vertical components. This vertical force resulted in a crack forming at the interface of the steel joist and the ECC slab, which consequently became the weak part of the cross-section due to the embedded steel joists (see Fig. 6a).

Beside the premature buckling and twisting of the steel substructure of specimen MP1, it was observed after testing had been terminated that cracks had begun to propagate from the corners of the embedded cast-ins directly below the quarter-points.

Testing of specimen MP2 resulted in a ductile failure mode, where the tension members began to yield at a total load of 110 kN (equivalent to an area load of 11 kN/m^2) and ultimately reaching 140 kN (equivalent to 15 kN/m^2) before testing was terminated. The tension member yielded over a 4.0 m mid-span section between the quarter points where the moment and consequently the tensile force in the cross-section of the truss was highest. The 4.0 m yield zone is furthermore restrained due to the additional stiffness of the replaced diagonals on each side of the yield zone.

At reaching the ultimate loading capacity, the cracking in the vicinity of the cast-in anchors had increased slightly and some flexural cracks had formed on the bottom side of the ECC slab at mid-span of the deck panel (Fig. 21).

As a result of the slip observed during testing of specimen MP3, a bolt in the bolted truss substructure sheared, causing the failure of the specimen. From about 60 kN (70 mm deflection) up to failure, the load–deflection response of MP3 is linear (Fig. 16), indicating that no slip occurred during that load interval. Furthermore, this linear response implies that the composite stiffness of MP3 is slightly less than that of MP4.

Testing of specimen MP4 was stopped once the element had exhibited a combination of a flexural and compression failure directly at the point of loading (quarter points) (Fig. 22). Prior to this failure, the interlocking connection between the steel truss and single-channel cast-in anchors had reached its ultimate load capacity and slipped, resulting in cracking of the ECC slab directly above the supports and bending of the end diagonal (Fig. 23). This slip in MP4 can be seen in Fig. 16 as relatively small drops in the load from 80 mm to about 230 mm deflection of the deck panel.

Both the slip in the bolted truss structure of MP3 and the slip in the interlocking connection between truss and embedded anchors of MP4 (as seen in Fig. 16) were clearly audible as acoustic events during testing.

6. Conclusions

An investigation of the structural behavior of prefabricated, light-weight composite deck elements, composed of high performance fiber reinforced cementitious composite and a steel substructure was presented in this paper. Two types of deck elements, the Integrally Cast Panels (ICPs) and the Modular Panels (MPs), were studied and compared.

The integrally cast panel design utilizes the simplicity of thin walled steel joists integrally joined with an ECC slab to form a deck panel. The modular panel concept expands on the benefits of the ICP by embedding anchors into the ECC deck slab, which are subsequently used to attach a steel truss substructure.

During the experimental program, the load–deflection behavior of both types of panels was shown to be consistent with predicted results and the failure modes were found to be ductile. Furthermore, it was demonstrated that by altering the steel truss substructure desired changes in the structural response can be achieved.

The deflections and natural frequencies of both types of panels were found to be within acceptable limits. The dynamic properties of the tested specimens were shown to meet typical structural performance requirements, however, additional research is needed to further improve the dynamic behavior towards higher natural frequencies and improved damping.

Both the ICP and MP concept offer the flexibility of adapting to a multitude of different performance requirements by selection of a specific combination of ECC deck and steel substructure, thereby controlling the strength and stiffness properties of the panel. Furthermore, the integrally cast and the modular concept with the embedded anchors allow the ECC slab and the attached substructure to behave as one composite element during loading.

The benefits of using a strain hardening concrete such as ECC are most evident in the tensile loading capacity and ductility of ECC which can eliminate transverse steel reinforcement and enables a ductile failure mode of the panel. However some transverse steel reinforcement could be provided for redundancy and safety. Furthermore, the significantly reduced amount of cementitious material and the high amount of recycled materials such as fly-ash (about 45% by weight) in ECC leads to reduced natural resource demands.

The design concept of both the ICP and the MP system offer a 70% weight reduction in comparison to hollow core decks while meeting structural performance requirements. Due to the layout of individual anchor points in the modular panels, shrinkage deformations of ECC do not cause initial deflections in the modular floor panel concept.

To meet fire resistance requirements for the presented design concepts, a few methods have been proposed for a similar structural floor concept [11]. For example, by placing gypsum boards under the steel substructure and thus isolating both the steel structure and the ECC slab from fire, or by spray-applying a fire-resistance material directly onto the substructure and ECC slab. Both approaches have been tested and rated for 1–3 h fire-resistance, depending on the thickness of gypsum boards or applied spray-on layer. Such fire resistance measures would also improve the acoustic resonance of the design.

A detailed study of the long-term behavior of the composite panels influenced by creep of the ECC slab, cyclic loading under service conditions and shear capacity is currently under way. In this context, due to the lack of conventional reinforcements and thin ECC slab design, punching shear needs to be examined particularly to further develop the concept and pursue commercialization.

References

[1] Naaman AE, Reinhardt HW. Proposed classification of HPFRC composites based on their tensile response. Mater Struct 2006;39(5):547–55.
[2] Lárusson LH, Fischer G, Jönsson J. Mechanical interaction of ECC reinforced with FRP rebar in tensile loading. In: Proceedings of advanced concrete materials. Stellenbosch, South Africa; 2009. p. 83–90.
[3] Fischer G. Fiber reinforced concrete for precast applications: an overview on recent developments and applications. In: International concrete conference & exhibition. ICCX. Cape Town, South Africa; 2007. p. 56–60.
[4] FIP Recommendations. Precast prestressed hollow core floors. 2 CEN European Committee for Standardisation. London (UK): Thomas Telford; 1988. p. 1–31.
[5] Martin LD, Perry CJ. PCI design handbook: precast and prestressed concrete. 6th ed. CA (USA): Precast/Prestressed Concrete Institute; 2004.
[6] Ching FDK. A visual dictionary of architecture. NY (USA): John Wiley and Sons; 1995. p. 203–6.
[7] Knudson B. Alternative concrete. Construction-Today Magazine; March 2009. p. 106–7.
[8] Schnellenbach-Held M, Pfeffer K. Punching behavior of biaxial hollow slabs. Cem Concr Compos 2002;24(6):551–6.
[9] Abramski M, Schnell J, Albert A, Pfeffer K. Experimental and numerical investigation of the bearing behaviour of hollow core slabs. Beton Stahlbetonbau 2010;105(6):349–61.
[10] Porter ML, Ekberg CE. Design recommendations for steel deck floor slabs. J Struct Div 1976;102(11):2121–36.
[11] Hambro. Hambro Technical Manual (Canada): Composite floor systems. Technical Publications; 2009. <http://www.hambro-floors.ws> [02.09.11].
[12] Kuhlmann U, Schanzlig J. A timber–concrete composite slab system for use in tall buildings. Struct Eng Int 2008;18(2):174–8.
[13] Lárusson L, Fischer G, Jönsson J. Mechanical interaction between concrete and structural reinforcement in the tension stiffening process. In: Proceedings of HPFRCC-6, Michigan, USA; 2011.
[14] Wang S, Li VC. Polyvinyl alcohol fiber reinforced engineered cementitious composites: material design and performances. In: Proceedings of international workshop on HPFRCC in structural applications. Honolulu, Hawaii; 2005. p. 104–11.
[15] Li VC, Fischer G. Reinforced ECC – an evolution from materials to structures. In: Proceedings of the first FIB congress, Osaka, Japan; October 2002. p. 105–22.
[16] Fischer G, Li VC. Influence of matrix ductility on the tension-stiffening behavior of steel reinforced Engineered Cementitious Composites (ECC). ACI Struct J 2002;99(1):104–11.
[17] Chopra AK. Dynamics of structures, theory and applications to earthquake engineering. 3rd ed. Prentice Hall; 2007. p. 48–50.
[18] Comité Euro-international du Béton. Vibration problems in structures: practical guidelines. Contribution à la 28.session plénière du CEB. Vienna; 1991.
[19] Flarus NV. "Concrete". "Stamped hollow core Damman Croes.jpg"; 2005. <http://www.flarus.com/Concrete.html> [08.04.11].
[20] United States Department of Transportation – Federal Highway Administration. "Focus – Desember 2003". "ibeams.jpg"; 2003. <https://www.fhwa.dot.gov/publications/focus/03dec/03.cfm> [08.04.11].
[21] Borecki M. "Filigran floor". "plyta6.jpg"; 2011. <http://www.marekborecki.pl/plyty_en.php> [08.04.11].
[22] RLSD. Richard Lees Steel Decking. "Ribdeck AL". From technical manual; 2008. <http://www.rlsd.co.uk/pages/ribdeck-al.php> [20.08.08].